TLR4-Binding DNA Aptamers Show a Protective Effect against Acute Stroke in Animal Models

Gerónimo Fernández,[1,7] Ana Moraga,[2,3,7] María I. Cuartero,[2,3,7] Alicia García-Culebras,[2,3] Carolina Peña-Martínez,[2,3] Jesús M. Pradillo,[2,3] Macarena Hernández-Jiménez,[4] Silvia Sacristán,[5] M. Irene Ayuso,[6] Rafael Gonzalo-Gobernado,[6] David Fernández-López,[2,3] M. Elena Martín,[5] María A. Moro,[2,3] Victor M. González,[5] and Ignacio Lizasoain[2,3]

[1]Aptus Biotech SL, Avda. Cardenal Herrera Oria 298, 28035 Madrid, Spain; [2]Unidad de Investigación Neurovascular, Departamento de Farmacología y Toxicología, Facultad de Medicina, Instituto Universitario de Investigación en Neuroquímica, Universidad Complutense de Madrid, 28040 Madrid, Spain; [3]Instituto de Investigación Hospital 12 de Octubre (i+12), 28041 Madrid, Spain; [4]Aptatargets SL, Avda. Cardenal Herrera Oria 298, 28035 Madrid, Spain; [5]Laboratorio de Aptámeros, Departamento de Bioquímica-Investigación, IRYCIS-Hospital Ramón y Cajal, 28034 Madrid, Spain; [6]Grupo de Investigación Neurovascular, Instituto de Biomedicina de Sevilla, IBiS/Hospital Universitario Virgen del Rocío/CSIC/Universidad de Sevilla, Avda. Manuel Siurot s/n, 41013 Sevilla, Spain

Since Toll-like receptor 4 (TLR4) mediates brain damage after stroke, development of TLR4 antagonists is a promising therapeutic strategy for this disease. Our aim was to generate TLR4-blocking DNA aptamers to be used for stroke treatment. From a random oligonucleotide pool, we identified two aptamers (ApTLR#1R, ApTLR#4F) with high affinity for human TLR4 by systematic evolution of ligands by exponential enrichment (SELEX). Optimized truncated forms (ApTLR#1RT, ApTLR#4FT) were obtained. Our data demonstrate specific binding of both aptamers to human TLR4 as well as a TLR4 antagonistic effect. ApTLR#4F and ApTLR#4FT showed a long-lasting protective effect against brain injury induced by middle cerebral artery occlusion (MCAO), an effect that was absent in TLR4-deficient mice. Similar effects were obtained in other MCAO models, including in rat. Additionally, efficacy of ApTLR#4FT in a model of brain ischemia-reperfusion in rat supports the use of this aptamer in patients undergoing artery recanalization induced by pharmacological or mechanical interventions. The absence of major toxicology aspects and the good safety profile of the aptamers further encourage their future clinical positioning for stroke therapy and possibly other diseases in which TLR4 plays a deleterious role.

INTRODUCTION

Stroke is a devastating illness, being the second cause of death and disability worldwide after cardiac ischemia. Currently, thrombolysis with tissue plasminogen activator (t-PA) is the only effective pharmacological therapy for the acute phase of stroke but, owing to the narrow therapeutic window of less than 4.5 hr and safety concerns, fewer than 5% of stroke patients are eligible for this treatment, reaching an effective reperfusion in approximately 50% of them. Therefore, stroke remains an enormous therapeutic challenge.

The Toll-like receptors (TLRs) are a family of pattern-recognition receptors initially identified for their role in the activation of innate immunity that can also control the activation of adaptive immune responses.[1,2] TLRs play a role in multiple pathologies even in the absence of infection. Specifically, TLR4, the first TLR characterized in mammals, has been involved in a large number of highly prevalent pathologies, such as stroke, acute myocardial infarction, atherosclerosis, sepsis, multiple sclerosis, acute and chronic pain, drug withdrawal, etc. Indeed, we and others demonstrated the implication of TLR4, a receptor with a fundamental role in the activation of innate immunity and in the inflammatory response elicited by an ischemic injury.[3–5] Since drugs able to modulate TLR4 are scarce, there is a growing interest in developing TLR4 agonists and antagonists for the treatment of different diseases in which this receptor plays a central role.[6–8]

Aptamers (from the Latin *aptus*, to fit, and the Greek *meros*, part or region) are single-stranded oligonucleotides selected from combinatorial libraries by systemic evolution of ligands by exponential enrichment (SELEX) technology. SELEX is used to identify DNA and RNA aptamers that recognize and selectively bind extra- and intracellular target molecules with high specificity and nanomolar affinity.[9–11] Once folded under physiological conditions, aptamers acquire unique three-dimensional structures based on their nucleotide sequence, being the tertiary structure of aptamers that confers the selectivity and affinity for their targets.[12–15] Aptamers offer the advantages of antibodies—high specificity and affinity—in a relatively small, chemically synthesized

Figure 1. Identification and *In Vitro* Pharmacodynamic Characterization of Aptamers with Higher hTLR4 Binding Affinity

(A) Graph showing binding of the selected aptamers to hTLR4 in ELONA assays. Data represent mean ± SEM of three independent experiments performed in triplicate. (B) Fold increase aptamer recovery after incubation of resin-hTLR4-protein complexes with ApTLR#1R and ApTLR#4F relative to RND40 (n = 3) by qPCR. (C) Fold increase aptamer recovery after incubation of 293-hTLR4A cells with ApTLR#1R and ApTLR#4F relative to HEK293 (n = 3) by qPCR. (D) SEAP assay for the characterization of the antagonistic effect of ApTLR#1R and ApTLR#4F on hTLR4. HB-hTLR4 cells were exposed to LPS (0.1 ng/mL; left) or DAMPs (5 µL; right) 1 hr prior to the addition of aptamers (0.2–200 nM) to the medium. Data are expressed as the percentage of SEAP activity relative to LPS or DAMPs alone (agonist control) (n = 9). Student's t test (*p < 0.05 versus agonist control).

such as ischemic stroke, due to their "rapid" pharmacokinetics and low toxicity profile. In this context, aptamers that specifically bind TLRs such as TLR9 and TLR2,[28,29] which modify the subsequent immune responses upon their activation, have been described.

We hereby report the discovery and characterization of novel aptamers capable to specifically bind and regulate TLR4 function. These aptamers have the potential to be effective inhibitors of TLR4-mediated signaling *in vitro* and *in vivo*, offering an effective and safe alternative treatment option for stroke and other diseases in which TLR4 plays an ethiopathogenic role.

RESULTS

DNA Aptamers Binding hTLR4 Show an Antagonistic Effect

In this work, we utilized two SELEX strategies in order to obtain specific aptamers against TLR4 able to block its activity. After six rounds of aptamer selection (described in the Materials and Methods section), a total of 14 non-redundant sequences were identified (Table S1). In the binding assays using enzyme-linked oligonucleotide assay (ELONA), ApTLR#1R, proceeding from the selection using recombinant protein, and ApTLR#4F aptamer, obtained from the selection using cells overexpressing TLR4, showed the highest binding capability to TLR4 recombinant protein (Figures 1A and S1).

Next, we analyzed the ability of ApTLR#1R and ApTLR#4F aptamers to bind the soluble TLR4 protein using qPCR, an alternative approach which allows us to quantify the presence of an aptamer bound to its target molecule. In this case, recombinant protein or cells

molecule free from cell-culture-derived contaminants. Aptamers are obtained by chemical synthesis, are non-immunogenic, and their smaller size allows more efficient entry into biological compartments. In addition, aptamers can be chemically modified to become extremely stable[14,15] or can be further truncated to eliminate oligonucleotide sequences that are not important for the interaction with the target or for the correct three-dimensional aptamer structure.[12,16] Consequently, they are currently being developed as agents for a wide array of applications, including biosensors, diagnostics, and therapeutics. Functional aptamers that antagonize the activity of several secreted targets[17–22] and cellular proteins[23–25] have been developed and several are currently under clinical testing.[26] Importantly, there is already an aptamer commercially available, pegaptanib, an RNA aptamer against vascular endothelial growth factor (VEGF), which is effective in treating choroidal neovascularization associated with age-related macular degeneration.[27] While therapeutic-oriented aptamers normally undergo modifications aimed to increase their resistance to degradation by nucleases and their half-life in circulation, unmodified single-stranded DNA (ssDNA) aptamers may present an optimal approach for the treatment of acute conditions
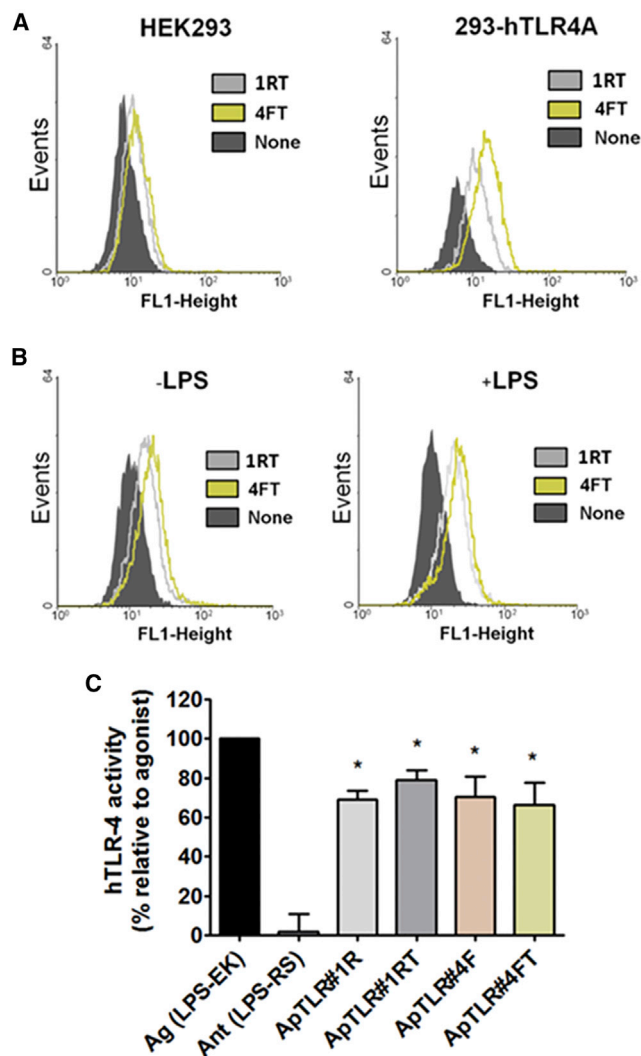
Figure 2. *In Vitro* Pharmacodynamics Characterization and Lead Optimization of Candidate Aptamers

(A) Representative flow cytometry charts showing fluorescence intensity (FL1-height) of human HEK293 (left) and 293-hTLR4A (right) cells incubated with 20 nM of Alexa 488-labeled aptamers (n = 3). (B) Representative flow cytometry charts showing fluorescence intensity (FL1-height) of 293-hTLR4A cells treated (right) or not (left) with LPS and incubated with Alexa 488-labeled aptamers as above (n = 3). (C) Characterization of the antagonistic activity of ApTLR#1RT, ApTLR#4FT, and their parent aptamers by SEAP assay (n = 6). Student's t test (*p < 0.05 versus agonist control).

overexpressing the TLR4 receptor are incubated with the aptamer and, after the corresponding washes, the aptamer bound is amplified by qPCR using the specific primers. Figure 1B shows the increase in aptamer recovery from the recombinant protein relative to the RND40 initial population. The results show that the threshold cycle (Ct) corresponding to the two selected aptamers is lower than that for the RND40 initial population, indicating that a higher amount of aptamers ApTLR#1R and ApTLR#4F is recovered.

In another set of experiments, the ability of aptamers to bind the TLR4 protein expressed in cells was analyzed. In these assays, ApTLR#1R and ApTLR#4F aptamers were added to 293-hTLR4A or HEK293T cells, and the aptamers recovered were used as templates in qPCR assays. Figure 1C shows the increase in recovery for each of the specific aptamers against TLR4 from cells that overexpress TLR4 (293-hTLR4A) with respect to cells that do not express the protein (HEK293T). As above, the results show that a greater amount of aptamers ApTLR#1R and ApTLR#4F bind to the surface of cells that overexpress TLR4, strongly suggesting a specific interaction with this receptor (Figure 1C).

We then explored whether the selected aptamers are able to affect TLR4 receptor activity. For this, HEK-Blue-hTLR4 cells were activated using the TLR4 agonist lipopolysaccharide (LPS) from *E. coli* K (LPS-EK) or DAMPs (molecular patterns associated to damage) obtained from cell lysis, and TLR4 activation was detected using a "secreted embryonic alkaline phosphatase" (SEAP) reporter gene. Our results show that both aptamers inhibited TLR4 activity (antagonist activity). From the concentration-response curve conducted for each aptamer (Figure 1D), we can conclude that the maximal antagonistic activity is obtained at 20 nM for both aptamers. An unspecific 38x(AG) aptamer did not produce any effect at the higher concentration. No agonistic effect was observed at any of the aptamer concentrations assayed.

Optimized Aptamers Maintain TLR4 Binding and Antagonistic Activity

Aptamers showing ability to inhibit TLR4 activity were modified by deleting specific regions of the sequence in order to increase their stability and, more importantly, to decrease their size. Thus, we designed the aptamers ApTLR#1RT and ApTLR#4FT, corresponding to the truncated forms of ApTLR#1R and ApTLR#4F, respectively (Figure S1). These new aptamers have structural motifs similar to the original ones, although with a higher theoretical free energy ($\Delta G = -4.61$ kcal/mol for ApTLR#1RT and $\Delta G = -2.13$ kcal/mol for ApTLR#4FT).

In order to check that optimized aptamers maintain the ability to bind TLR4, we performed flow cytometry assays to explore the binding of Alexa Fluor 488-labeled aptamers to 293-hTLR4A. Again, the parent human HEK293 cell line, lacking human TLR4, was used as a control. Figure 2A shows a peak shift relative to the control, indicating that the Alexa Fluor 488-labeled aptamers bind to 293-hTLR4A cells (Figure 2A, right), but not to HK293 cells (Figure 2A, left). In addition, our data show that ApTLR#4FT (Figure 2A, green line) binds to the target with higher affinity than ApTLR#1RT (gray line, Figure 2A). Interestingly, a slight increase in the fluorescence can be observed when cells are previously activated with LPS, relative to non-activated cells (median increase of 9.9 for ApTLR#1RT and 9.04 for ApTLR#4FT) (Figure 2B).

We also performed experiments to study the activity of the truncated forms of the aptamers. Our data show that both ApTLR#1RT and ApTLR#4FT maintain the antagonistic activity shown by their

A

B
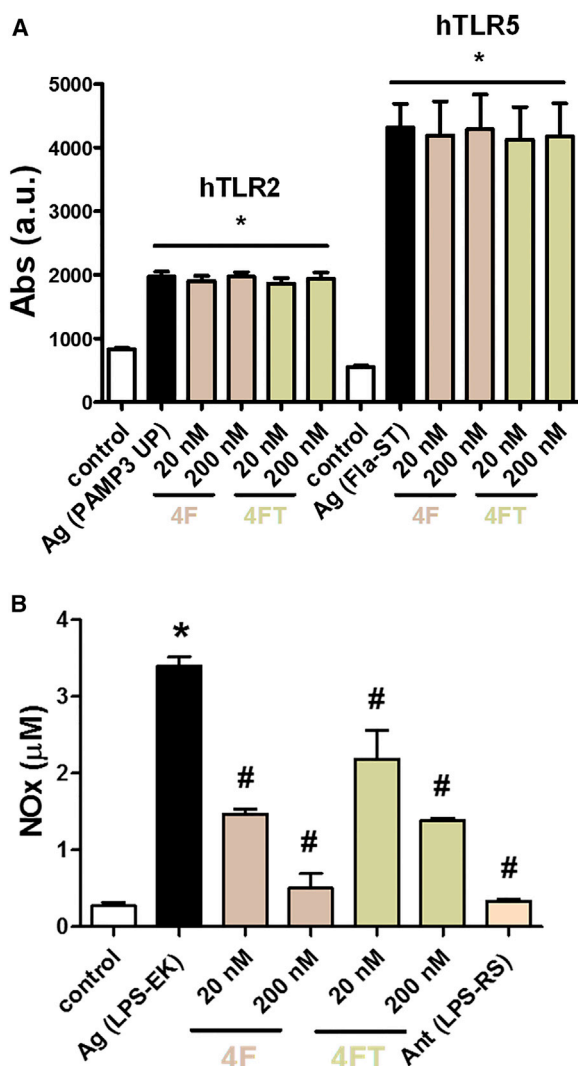
Figure 3. Pharmacological Characterization of ApTLR#4F and ApTLR#4FT
(A) Absence of antagonistic activity of ApTLR#4F and ApTLR#4FT (20 and 200 nM) on HB-hTLR2 and HB-hTLR5 cells activated with the selective TLR2 and TLR5 agonists Pam3 and Flat-ST. Data are expressed as SEAP activity compared to the control cells (n = 4). (B) Effect of the incubation of murine macrophages with ApTLR#4F and ApTLR#4FT (20 and 200 nM) 1 hr after LPS activation (500 ng/mL). Nitrites released to the incubation medium were quantified by the Griess reaction 24 hr after the addition of aptamers as an end-point marker of inducible nitric oxide synthase (iNOS) activity. Data represent mean ± SEM of three independent experiments performed in duplicate, two-way ANOVA followed by Bonferroni test. (*$p < 0.05$ versus control; #$p < 0.05$ versus LPS).

non-truncated precursors and exert their effect at the same extent as the original aptamers (Figure 2C).

ApTLR#4F and ApTLR#4FT Show TLR4-Specific Antagonistic Activity

In view of the lack of effect of ApTLR#1RT on infarct volume subsequently reported (Figure 4A), we decided to fully characterize

ApTLR#4F and ApTLR#4FT. First, we explored the specificity of the antagonist effect of ApTLR#4F and ApTLR#4FT against hTLR4 receptor by using the cell lines HB-hTLR2 and HB-hTLR5 with SEAP reporter gene. Cells were stimulated with their natural agonist, Pam3-up and FLA-ST, respectively, 1hr before the addition of the aptamers (20–200 nM). In this case, the aptamers used did not show any antagonistic effect on TLR2 or TLR5 receptors (Figure 3A).

Next, we confirmed the TLR4 antagonistic effect of these aptamers on peritoneal macrophages stimulated with LPS (500 ng/mL). Aptamers (20 and 200 nM) were added 1 hr after LPS treatment, and nitric oxide (NO) production was estimated as NO_x^- concentration in the medium after 24 hr of incubation with aptamers (Figure 3B). Our results show that both aptamers produce a concentration-dependent inhibition of NO_x^- release induced by LPS administration, although TLRApt#4F seems more active than TLRApt#4FT for the same concentrations.

ApTLR#4F and ApTLR#4FT Are Partially Resistant to Degradation and Do Not Produce Toxicity in Cells

The integrity of the aptamers in the presence of λ-exonuclease, DNase I, or human plasma was quantified. The results show that aptamers ApTLR#4F and ApTLR#4FT were resistant to λ-exonucleases even after 4 hr of incubation (Figure S2A). However, both aptamers were completely degraded after only 5 min incubation in the presence of DNase I in the assay conditions (Figure S2B). In addition, when aptamers were incubated in human plasma in physiological conditions, a time-dependent degradation was observed (Figure S2C).

In vitro toxicity was measured by 3-(4,5-dimethylthiazol-2-yl)-2,5-diphenyltetrazolium bromide (MTT) assay using two cell lines (HepG2 and HL-60) incubated with different concentrations of the aptamers (2–2,000 nM) for 24 and 48 hr. Our results show that a 20% of decrease in MTT activity in HepG2 cells and 35% in HL-60 cells was only observed at the highest concentration used after 24 hr of incubation (Figure S3). After 48 hr, the MTT activity was recovered, probably due to aptamer degradation.

ApTLR#4F and ApTLR#4FT, but Not ApTLR#1RT or 38x(AG), Reduce Infarct Volume after Stroke

In order to characterize the effect of aptamers on infarct volume after stroke, wild-type (WT) mice (C57BL/10J, expressing TLR4) subjected to permanent middle cerebral artery occlusion (pMCAO) were intraperitoneally (i.p.) treated with different doses of aptamers 10 min after the ischemic occlusion (Figure 4A). At 24 hr after pMCAO, WT mice treated with ApTLR#4F and ApTLR#4FT, but not with ApTLR#1RT, showed a significant reduction in the infarct volumes at 1 nmol when compared with WT-vehicle animals ($p < 0.05$; Figure 4A).

To discard non-specific effects, we performed some studies to determine the infarct volume in animals treated with 38x(AG) aptamer, which is an oligonucleotide consisting of a linear sequence containing 38 consecutive pairs AG, therefore useful as negative control. As
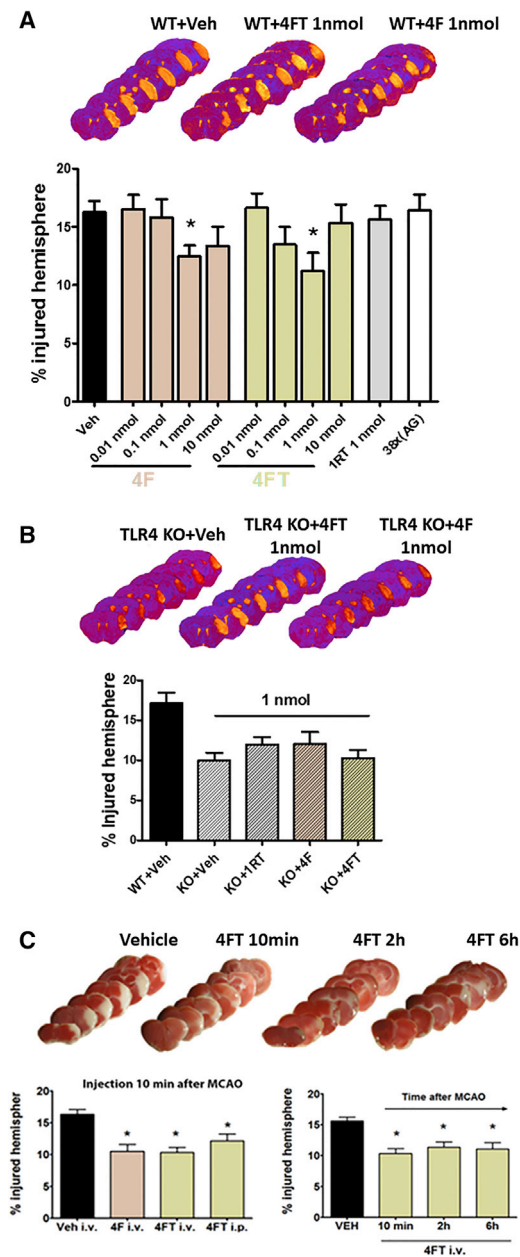
Figure 4. *In Vivo* Pharmacodynamics Characterization of the Protective Effect of Aptamers in Mice Subjected to Permanent Middle Cerebral Artery Occlusion

(A) Representative T2W MRI sequences showing the extent of brain infarction at 24 hr after pMCAO. Dose-response profile of ApTLR#4F and ApTLR#4FT administered i.p. 10 min after induction of pMCAO showing protective effect for 1 nmol (ApTLR#4F, n = 13) and 0.1 and 1 nmol doses (ApTLR#4FT, n = 8–9). ApTLR#1RT (n = 8) or 38x(AG) (as negative control of the aptamer; n = 8) did not affect lesion size. (B) Representative T2W MRI sequences showing the extent of brain infarction at 24 hr after pMCAO. Effect of ApTLR#4F (n = 8), ApTLR#4FT (n = 8), and ApTLR#1RT (n = 8) (1 nmol) on TLR4 knockout (KO) mice. (C) Representative TTC-stained sections at 24 hr after pMCAO in the therapeutic window study. Protective effect mediated by ApTLR#4F (n = 6) and ApTLR#4FT (n = 13) injected intravenously

observed in Figure 4A, animals treated i.p. with 38x(AG) 10 min after cerebral ischemia displayed similar infarct volumes to those observed in the vehicle-treated group determined 24 hr after ischemia by MRI.

To confirm that aptamer-induced reduction in infarct volume results from a specific effect on TLR4 receptor, TLR4 KO mice (C57BL/10ScNJ; mice lacking TLR4) exposed to pMCAO were also treated with 1 nmol of different aptamers. Our data show that, in this case, the size of the ischemic lesion in the groups treated with aptamers was no different from that found in the KO-vehicle group (Figure 4B), confirming that the effect of the aptamers is dependent on the presence of TLR4 receptor.

Since the intravenous (i.v.) route would be preferred for administration in stroke patients, we performed additional experiments in order to compare the effects of i.v. and i.p. administration of aptamers after stroke. WT mice subjected to pMCAO were treated with ApTLR#4F and ApTLR#4FT at 1 nmol 10 min after the occlusion by i.v. or i.p. route. At 24 hr after pMCAO, the reduction in infarct volume was similar after both routes (p < 0.05; Figure 4C). Considering that the average time frame of clinical intervention of patients after stroke onset is 2–4 hr, we studied the therapeutic window of protection mediated by ApTLR#4FT injected i.v., showing that the protective effect remains when aptamer is administered at 2 and 6 hr after pMCAO (p < 0.05; Figure 4C).

To study the distribution of ApTLR#4FT, we performed peripheral and central studies using Alexa Fluor 488-labeled ApTLR#4FT. First, we performed a flow cytometric analysis of aptamer in blood from $TLR4^{+/+}$ and $TLR4^{-/-}$ mice subjected to pMCAO that received an i.v. administration of Alexa Fluor 488-labeled ApTLR#4FT (1 nmol) 10 min after the surgery (n = 3–5). Basal and serial blood samples from tail were obtained at 5, 10, 15, and 30 min and 5 hr after aptamer administration. Our results demonstrate that ApTLR#4FT is detected in blood 5 min after the administration in pMCAO $TLR4^{+/+}$ mice (Figure S4A). However, in $TLR4^{-/-}$ mice, we did not detect aptamer binding at any of the times studied. Also, we found that Alexa Fluor 488-labeled ApTLR#4FT gated cells were mainly in the granulocyte region based on forward scatter (FSC) and side scatter (SSC) gating strategy (Figure S4B).

We have also found that ApTLR#4FT was able to cross the blood-brain barrier and reach the ischemic brain region by fluorescence microscopy analysis of brain sections, showing Alexa Fluor 488-labeled ApTLR#4FT in cells located within the core region of the ischemic lesion in mouse brain tissue (Figure S4C, green). Signal specificity was confirmed by incubation with Cy3-conjugated anti-Alexa 488 antibody (Figure S4C, red). Unconjugated ApTLR#4FT was used as negative control (Figure S4D).

10 min after pMCAO. Window of protection mediated by ApTLR#4FT given intravenously after pMCAO (n = 6). Data represent mean ± SEM. Non-parametric, one-way Kruskal-Wallis ANOVA with Dunn's post-hoc test (*p < 0.05 versus pMCAO + vehicle).
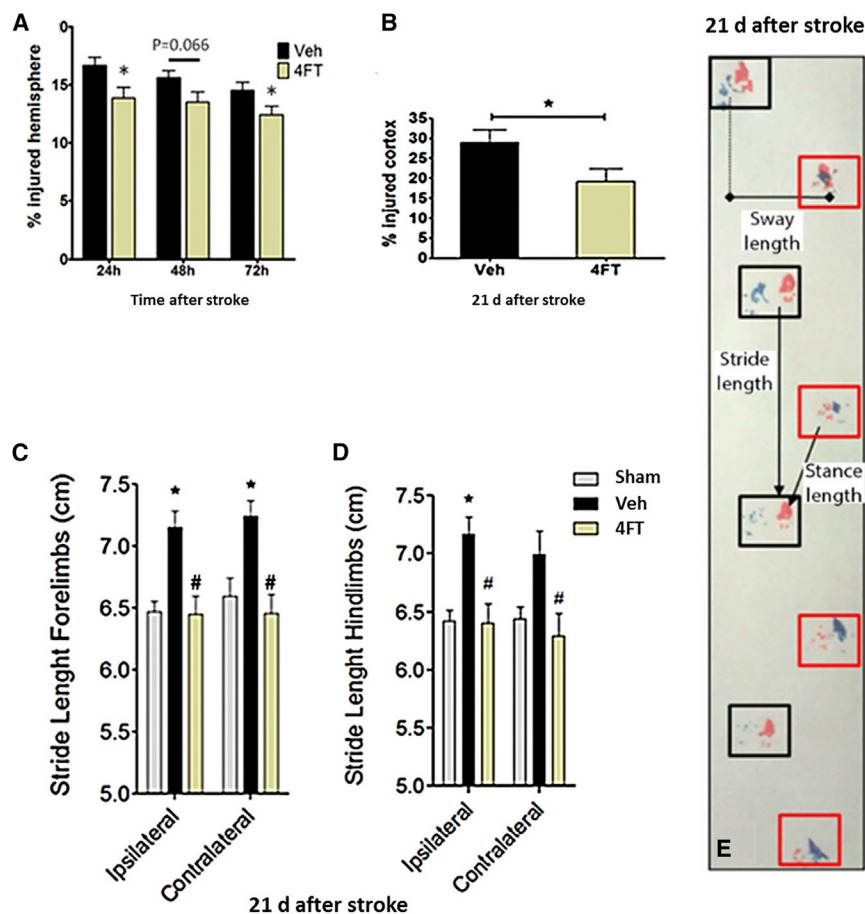
Figure 5. Characterization of the Protective Effect of ApTLR#4FT in the Long-Term

(A) Reduction of infarct size mediated by ApTLR#4FT (1 nmol) measured longitudinally by T2WI-MRI was sustained at 72 hr after pMCAO (n = 21). (B) Quantification of % of injured cortex performed on Nissl-stained serial sections showed long-lasting permanence of protection mediated by ApTLR#4FT (n = 10) at 21 days after pMCAO. (C and D) Assessment of neurological function by the footprint test at 21 days after pMCAO showed a normalization of the stride length in forelimbs (C) and hindlimbs (D) induced by ApTLR#4FT (n = 10). (E) Representative depiction of the distances measured in the footprint test. Data represent mean ± SEM, two-way ANOVA followed by Bonferroni test for (A), (C), and (D). *p < 0.05 versus Veh or sham; #p < 0.05 versus ipsilateral. Student t test for (B) (*p < 0.05 versus Veh).

ApTLR4#4FT (1 nmol) or vehicle were tested. No effects were observed on parameters related to muscular tone, coordination, and sensorimotor responses. However, an alteration of the performance of mice in the open-field test was noted. Mice injected with ApTLR4#4FT spent more time in the periphery of the field (Figures 6A and 6B) in detriment of exploration of the central area (Figures 6A and 6C). This is normally interpreted as a sign of higher anxiety after exposure to a new environment. Likewise, a transient decrease in animal's weight was detected at 24 hr, which was reverted at 48 hr. Further additional anxiety tests need to be performed to confirm the presence of an anxiogenic effect of ApTLR4#4FT.

Finally, the effect of i.v. administration of aptamers or vehicle on physiological parameters was explored. Administration of ApTLR4#4FT or ApTLR4#4F showed no effect on any of the parameters measured when compared to vehicle administration (Figure 6D). In addition, ApTLR4#4FT did not produce any *in vivo* toxic effects in a wide variety of tissues and organs studied, including liver (data not shown).

ApTLR#4FT Produces a Long-Term Reduction of the Infarct Volume and a Recovery of Neurological Function after pMCAO in Mice

Since clinical evaluation of novel therapies in stroke patients typically rely on a primary end-point for anatomical and functional improvement at 90 days after stroke, we explored in the long-term the persistence of the protective effect of ApTLR#4FT observed acutely. Longitudinal analysis using T2WI MRI showed a sustained reduction of brain infarction up to 72 hr after stroke (Figure 5A). Long-lasting permanence of the acute protective effect of ApTLR#4FT was observed at 21 days after pMCAO, a time when infarct is considered stable in mice (Figure 5B). A correlation with a recovery of neurological function was also observed in the footprint test (Figure 5E) as a reduction in the stride length of forelimbs (Figure 5C) and hindlimbs (Figure 5D) as a result of the acute treatment with ApTLR#4FT.

ApTLR#4F and ApTLR#4FT Do Not Produce Neurotoxic or Physiological Effects

Neurotoxicity *in vivo* was evaluated by using the modified Irwin test, a battery of tests classically used for assessment of the presence of neurotoxic effects derived from drugs.[30] Naive mice injected with

ApTLR#4FT Reduces the Infarct Volume in Other Stroke Models: Mechanisms Involved
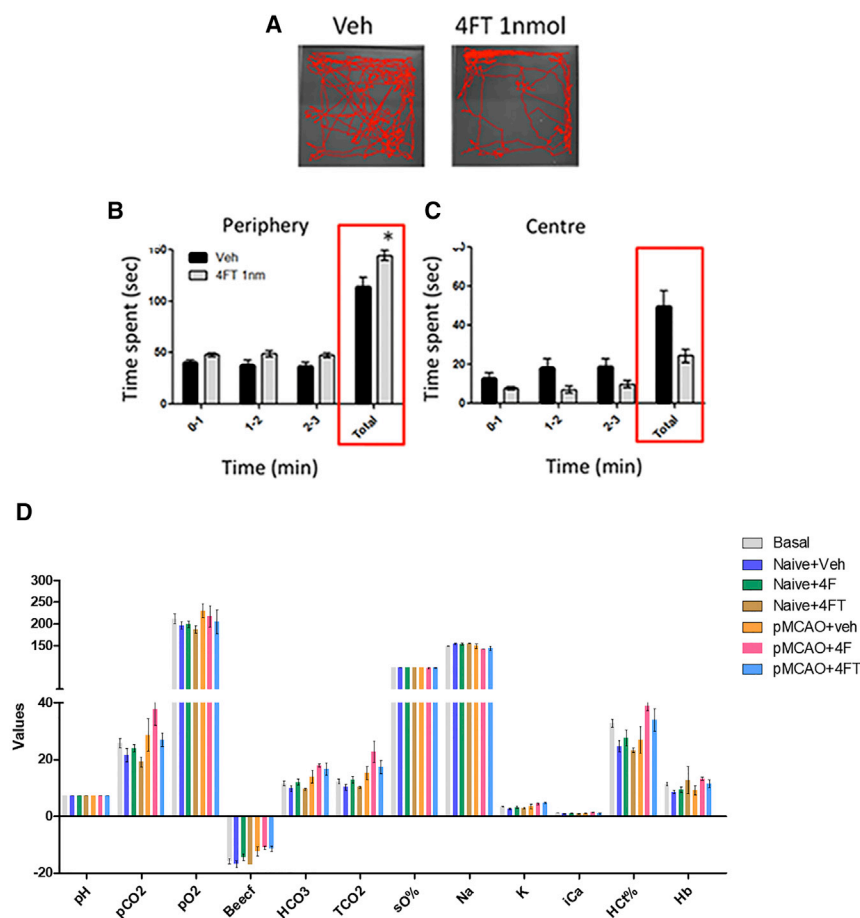
Therapeutic potential of ApTLR#4FT and ApTLR#4F was explored using another brain ischemia model with a proximal occlusion (affecting cortex and striatum) and involving reperfusion (intraluminal transient MCAO [tMCAO]; Figures 7A and 7B), in a different rodent species (rat). In this setting, only ApTLR#4FT showed significant protection over vehicle, while no effect of ApTLR#4F administration was observed (Figures 7A and 7B). Remarkably, protection achieved by ApTLR#4FT reached 49% reduction of infarct size, being considerably higher than that observed in the pMCAO model in mice. We

Figure 6. *In Vivo* Toxicity Assays of ApTLR#4F and ApTLR#4FT

(A) Representative depictions showing the trajectory of mice in the open-field test, as part of the Irwin battery. (B and C) Graphs showing the time spent by the mice in the periphery (B) and center (C) of the open field (n = 9), suggesting a higher level of anxiety in mice treated with ApTLR#4FT. Data represent mean ± SEM, two-way ANOVA followed by Bonferroni test (*p < 0.05 versus Veh or sham). (D) Graph showing the effect of intravenous administration of vehicle, ApTLR#4FT, and ApTLR#4F on a battery of physiological parameters measured in blood. No significant effect of ApTLR#4FT or ApTLR#4F (n = 6–9) was observed.

strate any significant differences between vehicle- and ApTLR#4FT-treated groups in number, area or integrated density of microglial cells in the peri-infarct area (Figures S5A and S5B). On the other hand, extravasated immunoglobulin G (IgG) area (indicating blood-brain barrier damage) was decreased in animals treated with ApTLR#4FT, 10 min after pMCAO, when compared with vehicle group (p < 0.05; Figure S6).

DISCUSSION

In this study, we have characterized an aptamer, ApTLR#4F, and its truncated form, ApTLR#4FT, which show antagonistic activity against TLR4 and, subsequently, a protective effect against experimental stroke, a setting where TLR4 plays a crucial role in the initiation of ischemic injury.

have also determined the neurological function using the motor score test up to 21 days after tMCAO, showing a significant protection at 2 and 7 days after stroke in rats treated with ApTLR#4FT (Figure 7C).

Likewise, we explored the effect of ApTLR#4FT in a third brain ischemia model (MCAO by electrocoagulation; Figure 7D) in mice. The administration of 1 nmol of ApTLR#4FT 10 min after injury also showed a significant and robust protection over vehicle, reaching 33% reduction of infarct size (Figure 7D).

We also used this model to study mechanisms involved in the protective effect of ApTLR#4FT, by performing a quantitative analysis of different plasma cytokines using a customized cytometric bead array (CBA) (see Materials and Methods). Treatment with the ApTLR#4FT significantly reduced the plasma levels of interleukin-6 (IL-6), IL-12p70, and interferon-γ (IFN-γ), but not of tumor necrosis factor (TNF), IL-10, or Monocyte Chemoattractant Protein-1 (MCP-1), at 24 hr after the ischemic insult, compared with the vehicle mice group (n = 8–15; p < 0.05) (Figure 7E).

Additionally, we studied microglial activation and blood-brain barrier damage after pMCAO in both groups. Our results did not demon-
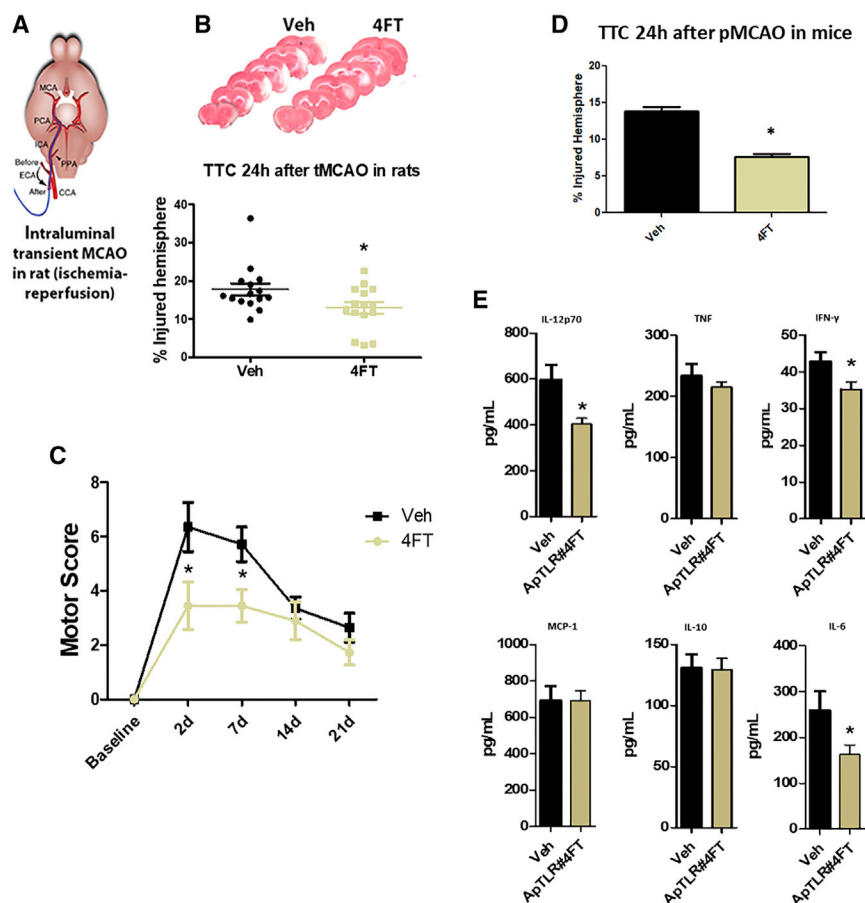
First, we identified two aptamers (ApTLR#1R and ApTLR#4F) against human TLR4 (hTLR4) by using the systematic evolution of ligand by exponential enrichment (SELEX) method, which show TLR4 antagonistic activity. Since it has been described that TLR4 functions can vary across different species and, in particular, between humans and rodents, it is important to emphasize that these aptamers are specific to human TLR4 (for review see Vaure and Liu[31]). In order to enhance their pharmacokinetic properties, we carried out a post-SELEX optimization to obtain their truncated (T) forms (ApTLR#1RT and ApTLR#4FT). For that, the aptamers were modified by deleting specific regions of the sequence after studying the secondary structures of aptamers and analyzing the ability of aptamers to form G-quadruplex structures. Aptamers must ideally have a high stability, important for applications in biological systems in order to reach their target proteins without being degraded. Many of the aptamers described in the literature contain G-quadruplex structures,[32–34] which strongly stabilize the tertiary structure. Interestingly, ApTLR#1RT exhibits relatively high free energy but, eventually, it would be able to form a G-quadruplex structure. However, our results

Figure 7. Study of the Mechanisms Involved in the Infarct Volume Reduction Produced by ApTLR#4FT in Other Stroke Models

(A) Depiction showing the surgical procedure for intraluminal tMCAO. (B) Representative TTC-stained sections at 24 hr after tMCAO in rats. Protection mediated by ApTLR#4FT (n = 15) given intravenously 10 min after reperfusion following tMCAO in rats. Data represent mean ± SEM. Non-parametric, one-way Kruskal-Wallis ANOVA with Dunn's post-hoc test (*p < 0.05 versus Veh). (C) Assessment of neurological function by the motor score test up to 21 days after tMCAO showed a significant protection at 2 and 7 days after stroke induced by ApTLR#4FT (n = 10). Data represent mean ± SEM, two-way ANOVA followed by Bonferroni test (*p < 0.05 versus Veh). (D) Protection mediated by ApTLR#4FT (n = 8–15) given i.p. 10 min after pMCAO by electrocoagulation in mice and (E) effects of ApTLR#4FT on plasma protein levels of inflammatory mediators after pMCAO in mice. Protein levels were determined 24 hr after pMCAO by cytometric bead array. Samples were tested in duplicate (n = 8–15 in each group). Data are expressed as mean ± SEM, Student's t test (*p < 0.05 versus Veh).

show that ApTLR#4FT is able to bind to the target with higher affinity than ApTLR#1RT, although both truncated aptamers maintain similar structural motifs and antagonistic activities as their non-truncated precursors.

We focused our study on ApTLR#4F and its truncated form ApTLR#4FT, for which subsequently discussed studies showed a neuroprotective decrease in infarct volume after experimental stroke. The human TLR family can be divided into extracellular members, TLR1, TLR2, TLR4, TLR5, TLR6, and intracellular members, TLR3, TLR7, TLR8, and TLR9. Upon ligand binding, TLR4 and TLR5 form homo-dimers, whereas TLR2 forms hetero-dimers with TLR1 or TLR6.[35] We have confirmed the specificity of our aptamers against TLR4 by analyzing the effect on extracellular TLR2 and TLR5 which, moreover, form homo-dimers (TLR5) and hetero-dimers (TLR2). Our results show that none of these aptamers exerts any effect on TLR2 or TLR5, confirming the specificity for TLR4.

Regarding stability, we have found that both aptamers are degraded at different times after incubation with human plasma. It is interesting to point out that aptamers aimed at the treatment of acute diseases could be degraded after a short period to prevent unwanted toxic effects.

Importantly, we have studied the effect of ApTLR#4F and ApTLR#4FT on infarct volume after ischemic stroke, a disease in which we and others have demonstrated the key role of TLR4 in the brain damage associated to this pathology. We showed that TLR4-deficient mice have smaller infarctions and less inflammatory response after an ischemic insult.[3,4] Furthermore, the exogenous administration of the TLR4 antagonist TAK-242 also protected brain from acute damage induced by intracerebral hemorrhage[36] and by ischemic injury.[37] Now, our present data show that the post-stroke administration of both aptamers produces a remarkably neuroprotective effect by decreasing infarct volume.

Interestingly, this effect is TLR4 dependent, because none of them showed any effect on TLR4-deficient mice. The long-lasting protection mediated by ApTRL#4FT at 21 days, as well as the correlation of the anatomical infarct size reduction with the functional recovery, adds a critical translational value to the results, since these endpoints mimic clinical endpoints and timing of monitoring in stroke patients. In this context, it has been demonstrated[5] that TLR4 is active long enough after stroke to act effectively with drugs that block TLR4-signaling response. In addition, there is a release and secretion of DAMPs from dying cerebral tissue after stroke (for review, see Bustamante et al.[38]) that activate these receptors, thereby triggering the inflammatory response.

We have also demonstrated that ApTLR#4FT, administered after the onset of ischemic injury, diminishes the plasma protein levels of several pro-inflammatory molecules (IL-6, IL-12p70, and IFN-γ)

and reduces the blood-brain barrier disruption, effects that could be involved on the protective effect found.

Importantly, the efficacy of ApTLR#4FT in a model of brain ischemia-reperfusion in rat supports the use of this aptamer in patients undergoing artery recanalization induced by pharmacological (thrombolysis) or mechanical (endovascular thrombectomy) interventions, as an adjuvant therapy in patients in whom recanalization does not lead to major recovery. The absence of major toxicological aspects and the good safety profile characterized for ApTLR#4FT and ApTLR#4F further encourage their future clinical positioning for stroke therapy.

Other aptamers against TLRs have been also developed. Thus, Watanabe et al.[39] isolated two RNA aptamers against human TLR3 with high affinity in TLR3-transfected HEK293 cells. Later, Wu et al.[28] demonstrated the *in vivo* efficacy of a phosphodiester TLR9 aptamer and its beneficial effect in a pulmonary anthrax infection model. Chang et al.[29] also described an aptamer, AP177, that can effectively antagonize TLR2, inhibit nuclear factor κB (NF-κB) activity, and reduce cytokine secretion by >80%, showing therapeutic potential in the treatment of diseases related with deregulated TLR2 immune responses.

The two new aptamers described herein provide a novel and powerful therapeutic strategy for stroke. Before aptamers can be used in humans, several additional tests will need to be performed in animal models, including biodistribution and dose-response analyses. Once the parameters of pharmacokinetics and dynamics are determined in animal models, we envision that the aptamers could be tested in human clinical trials, perhaps first in patients who are treated with tPA. In addition, the great affinity and specificity shown by the aptamers, together with their advantages when compared with traditional drugs or antibodies (safety, stability, *in vitro* selection, ability to be modified without structural alterations, production costs, etc.) makes them excellent candidates for their incorporation into the therapeutic arsenal not only for stroke but also for other diseases in which TLR4 plays a deleterious role.

MATERIALS AND METHODS
Cell Lines and Reagents
Five different cell lines, HEK293, 293-hTLR4A, HEK-Blue-hTLR4, HEK-Blue-hTLR2, and HEK-Blue-hTLR5 cells, were used in this study. HEK293 cells are human embryonic kidney epithelial cells. 293-hTLR4A cells were obtained by stable transfection of the hTLR4a gene (InvivoGen, San Diego, CA, USA). HEK293 cells were cultured in DMEM supplemented with 10% fetal bovine serum (FBS) (Life Technologies, Inc., Carlsbad, CA, USA), 10 U/mL penicillin, and 100 μg/mL streptomycin (Gibco). 293-hTLR4A cells were cultured in the same medium supplemented with 10 μg/mL blasticidin (Sigma-Aldrich, St. Louis, MO, USA).

HEK-Blue-hTLR4 (InvivoGen # hkb-htlr4) were obtained by co-transfection of the hTLR4 receptor and MD-2/CD14 co-receptor genes into HEK293 cells. The cells were cultured in DMEM supplemented with 10% FBS, 10 U/mL penicillin, and 100 μg/mL streptomycin and (1×) HEK-Blue Selection (InvivoGen, San Diego, CA, USA). HEK-Blue-hTLR2 (InvivoGen #hkb-htlr2) and HEK-Blue-hTLR5 (InvivoGen #hkb-htlr5) were obtained by co-transfection hTLR2 and hTLR5 receptor genes, respectively, and SEAP reporter gene into HEK293 cells. These cells were cultured with the same medium that HEK-Blue hTLR4 cells supplemented with (1×) Blasticidin (InvivoGen ref, ant-bl-1) for HEK-Blue-hTLR2 cells and (1×) Zeocin (Invivogen ref, ant-zn-1) for HEK-Blue-hTLR5 cells.

Primers and Aptamers
The ssDNA library composed of 40-nucleotide (nt) randomized probe sequences flanked by 18-nt PCR priming sequences at both the 5′ and the 3′ ends (5′-GCGGATGAAGACTGGTGT-[N]40-GCCCTAAA TACGAGCAAC-3′), named RND40, and all other labeled and non-labeled primers and aptamers were synthesized by IBA (Gottingen, Germany). The bound sequences, isolated during the SELEX process, were amplified by PCR primers with the sequences 5′-GCGGATGAA GACTGGTGT-3′ (F3) and 5′-GTTGCTCGTATTTAGGGC-3′ (R3). To ensure proper folding, aptamers were denatured at 95°C for 10 min, cooled to 4°C for 10 min, and then used at 37°C until used.

Expression and Purification of Recombinant Human TLR4
Coding sequence for mature recombinant human TLR4 (rhTLR4) (Glu24-Lys631) was cloned in pFastBacI vector and the recombinant construct transformed in DH10Bac cells. Recombinant hTLR4 fused to a 6xHis tail at the C-terminal end was expressed in Sf9 cells and purified by affinity chromatography on niquel-nitrilotriacetic acid (Ni-NTA) resin columns using ÄKTA Prime. The predicted molecular weight of rhTLR4 is 70.1 kDa.

Aptamer Selection: Cell-SELEX and Protein-SELEX
Two selection procedures using hTLR4-expressing HEK293T cells (293-hTLR4A, InvivoGene) (cell-SELEX) or HIS-tagged hTLR4 protein (protein-SELEX) have been performed. In the first round of the cell-SELEX, intact hTLR4-expressing HEK293T cells were plated in a p96 plate and incubated in culture medium with 1 nmol of ssDNA RND40 library previously folded in SELEX buffer (20 mM Tris-HCl [pH 7.4]; 150 mM NaCl; 1 mM MgCl$_2$) at 37°C for 1 hr (rounds 1–3) or 30 min (rounds 4–6). The cells were washed twice with PBS and then recovered and used as template for aptamer amplification. The aptamers were amplified using F3 and R3 primers in PCR buffer under the conditions of 1 μM/primer, 250 μM deoxinucleoside triphosphates (dNTPs), in a final volume of 100 μL. Contraselection steps were performed before the initial round and after rounds three and six of the SELEX procedure with HEK293 cells.

The protein-SELEX procedure was performed as previously described.[13] In brief, 1 nmol of structured RND40 population was mixed with 100 pmol of rhTLR4 and incubated in SELEX buffer as above. The bound aptamer-hTLR4 complexes were purified using Ni-NTA superflow (QIAGEN, Madrid, Spain). Contraselection steps were performed before the initial round and after rounds three and six

of the SELEX procedure with Ni-NTA superflow resin (Supplemental Materials and Methods).

Aptamer Cloning, Sequencing, and Secondary Structure Prediction

After six rounds, the selected aptamer populations were amplified by using 1 U Taq DNA polymerase (Biotools) in 50 μL of reaction also containing 1× PCR buffer, 125 mM dNTPs, 1 μM F3 primer, and 1 μM R3 primer. The dsDNA product with "A"-overhangs was cloned into pGEM-T Easy-cloning vector (Promega) following manufacturer's instructions. Individual clones were sequenced using T7 (5′-TAATACGACTCACTATAGGG-3′) and Sp6 (5′-ATTTAGGTGA CACTATAGAA-3′) primers. Selected ssDNA molecules were subjected to secondary structure prediction using the mFold version 3.5 software (http://unafold.rna.albany.edu)[40] at 37°C in 150 mM NaCl and 1 mM MgCl₂ and QGRS Mapper (http://bioinformatics.ramapo.edu/QGRS), a web-based server for predicting G-quadruplex in nucleotide sequence.[41]

ELONA

ELONA was used to screen aptamers binding to rhTLR4 protein as described.[13] In brief, 200 μL of the solution (5 μg/mL, 71 pmol/mL) of rhTLR4 protein in SELEX buffer with 0.2% BSA were added to a 96-well microtiter plate (NUNC) and incubated overnight at 4°C. Afterward, digoxigenin-labeled aptamers were diluted in SELEX buffer at 500 ng/mL (20 nM), denatured for 10 min at 95°C, and cooled for 10 min on ice. Then, 200 μL of the solution were added to each well, and the plate was incubated at 37°C for 1 hr, after which individual wells were washed four times with SELEX buffer to remove unbound ssDNA. Next, 200 μL of a 1/1,000 dilution of anti-digoxigenin antibody conjugated with horseradish peroxidase (POD) (Roche) were added to the individual wells. Following 30 min incubation at room temperature on a shaking platform, the plates were washed four times and developed using 2,2'-azino-bis(3-ethylbenzothiazoline-6-sulphonic acid) (ABTS) solution (Boehringer-Mannheim) according to the manufacturer's instruction. Optical density (OD) values at 405 nm were determined using a microplate reader from TECAN.

Binding Affinity Assays

To confirm the binding of the selected aptamers to the target, the recombinant protein or cells expressing hTLR4 were incubated with the aptamers and the bound aptamers amplified by qPCR. In a first set of experiments, rhTLR4 protein was bound to Ni-NTA agarose resin (QIAGEN). Twenty microliters of resin containing 70 ng (1 pmol) of rhTLR4 protein were incubated with 12.5 ng (0.5 pmol) of each aptamer in a final volume of 500 μL of PBS complemented with 1 mM MgCl₂ at 37°C for 10 min. Afterward, individual wells were washed four times with SELEX buffer to remove unbound ssDNA and resin-rhTLR: aptamer complexes were recovered by centrifugation at 10,000 × g for 5 min in 50 μL H₂O. In another set of experiments, HEK293 and 293-hTLR4A cells were plated in P96 multiwell plates (10,000 cells/well). After 6 days, 500 ng of previously folded aptamers were added to the cells and incubated for 30 min at 37°C. Cells were washed twice with PBS and recovered in 10 μL of PBS. In both cases,

the aptamers recovered were amplified by qPCR. Briefly, qPCR was performed on an iQ5 Cycler instrument (Bio-Rad) with Sybr green master mix (Biotools) according to the manufacturer's instructions. Specifically, for binding affinity assays, 20 μL reactions included 0.25 μM F3 and R3 primers and 2 μL (from experiments using soluble rhTLR4) or 10 μL (from experiments using rhTLR4-expressing cells) of the samples containing the aptamers. PCR was performed as follows: 95°C for 5 min; 25 cycles (95°C for 20 s; 57°C for 15 s; 72°C for 20 s).

Secreted Alkaline Phosphatase Assay for Screening TLR4 Antagonistic Effects of Aptamers

HEK-Blue-hTLR4 cells expressing hTLR4, MD2, and CD14 proteins were seeded onto 96-well culture plates at 2×10^4 cells/well. When the cells reached 70%–80% confluence, they were incubated with LPS-EK-ultra pure (InvivoGen, USA) at a concentration of 0.1 ng/mL or 5 μL of DAMPs, supernatant from 5×10^6 HEK293 cells lysed in 200 μL of H₂O and centrifuged 1 min at $10,000 \times g$, in a final volume of 190 μL. After 1 hr of incubation, 10 μL of aptamer diluted in SELEX buffer at several concentrations (0.2, 2, 20, and 200 nM) were added. LPS from *Rhodobacter sphaeroides* (LPS-RS; InvivoGen, USA) at a concentration of 200 ng/mL was used as an antagonist control. An oligonucleotide consisting of a linear sequence containing 38 consecutive pairs AG [38x(AG)] was used as a negative control. SEAP activity was measured after 24 hr using QUANTI-Blue substrate (InvivoGen, USA) at 630 nm. Cells incubated in the presence of the vehicle were used as a blank.

The specificity of aptamers ApTLR#4F and ApTLR#4FT was tested by SEAP assay. In these assays, we used the cell lines HEK-Blue-hTLR2 and HEK-Blue-hTLR5, stimulated with their natural agonist, Pam3-up (synthetic triacetilated lipoprotein ultrapure; InvivoGen#tlrl-pam) at 0.1 ng/mL and FLA-ST (flagelin from *S. typhimurium* ultrapure; InvivoGen ref, tlrl-stfla) at 50 ng/ml, respectively, for 1 hr. Afterward, ApTLR#4F and ApTLR#4FT at 20 nM and 200 nM were added and the SEAP activity measured as above.

Effect of Aptamers on Nitric Oxide Release in RAW 264.7 Macrophages

Peritoneal macrophages were seeded in 12-well plates at a density of 1×10^6 cells/mL and were incubated with 500 ng/mL of LPS (Sigma) at 37°C for 20 hr. Aptamers were added 1 hr after LPS treatment at 20 or 200 nM final concentration. The release of NO into phenol red-free medium was determined from the amount of accumulated nitrite, measured spectrophotometrically with the Griess reagent at 24 hr after aptamers administration (Sigma, St. Louis, MO, USA). The absorbance at 548 nm was compared to a standard NaNO₂ solution.[42] Samples were assayed in duplicate.

Flow Cytometry Analysis

All flow cytometry analyses were performed on a FACScan model flow cytometer (Becton Dickinson Immunocytometry systems). Binding of aptamers to cell-surface TLR4 was analyzed by seeding

HEK293 or HEK-Blue-hTLR4 cells onto 24-well culture plates at 2×10^5 cells/well in 200 μL complete DMEM supplemented with HEK-Blue Selection buffer. Afterward, cells were incubated in the absence or presence of the TLR-4 activator LPS-EK-ultrapure (LPS-EK-UP) (0.4 ng/well) for 30 min and then with the Alexa Fluor 488-labeled aptamers (20 nM) in 50 μL volume of PBS buffer containing 1 mM $MgCl_2$ and 1 mg/mL BSA for 30 min at room temperature in the dark. Cells were then washed and subjected to flow cytometry analysis.

Animals

Adult male mice C57BL/10J (WT; mice expressing TLR4) and C57BL/10ScNJ (KO; lacking functional TLR4) (8–10 weeks) and adult male Sprague-Dawley (200–250 g) were obtained from The Jackson Laboratory. Animals were housed individually under standard conditions of temperature and humidity and a 12-hr light/dark cycle (lights on at 08:00) with free access to food and water. All procedures were carried out in accordance with ARRIVE guidelines and the European Communities Council Directive (86/609/EEC) and reviewed by the Ethics Committees on Animal Welfare of Universidad Complutense.

Experimental Groups

All groups were performed and quantified in a randomized fashion by investigators blinded to the specific treatments. Mice were subjected to a pMCAO. Animals received an i.p. or i.v. (tail vein, i.v.) administration of ApTLR#4F (0.01–1 nmol), ApTLR#4FT (0.01–1 nmol), ApTLR41RT (1 nmol), 38x(AG), or vehicle (PBS + 150 mM $MgCl_2$) 10 min, 2 hr, or 6 hr after pMCAO. Rats were subjected to tMCAO and received 0.59 mg/kg ApTLR#4F, 0.45 mg/kg ApTLR#4FT, or vehicle i.v. (tail vein, i.v.).

Induction of Permanent Focal Ischemia in Mice

Mice were subjected to a distal pMCAO through ligation of the MCA with a 9–0 suture just before its bifurcation into the frontal and parietal branches as previously described.[4] The ipsilateral common carotid artery was also permanently occluded. These experimental conditions led to moderately sized cortical infarcts. In other groups of mice, the middle cerebral artery (MCA) was also occluded permanently by the electrocoagulation method as previously described.[43] Mice were anesthetized with isoflurane 1.5%–2% in a mixture of 80% air/20% oxygen, and body temperature was maintained at physiological levels with a heating pad during the surgical procedure and anesthesia recovery. Following surgery, individual animals were returned to their cages with free access to water and food. Animals were sacrificed by an overdose of isoflurane. Physiological parameters were not significantly different among the different groups studied. No spontaneous mortality was found after pMCAO with this model in any experimental group.

Induction of Transient Focal Ischemia in Rats

Transient focal brain ischemia (tMCAO) was induced by intraluminal occlusion of the right MCA with reperfusion, as reported.[44] In brief, rats were anesthetized with isoflurane in a mixture of O_2 and N_2O (30:70) and intubated through the trachea for controlled ventilation. Mean arterial blood pressure was monitored, and body temperature was maintained between 36.5°C and 37.5°C during surgery. Briefly, the common and external carotid arteries were exposed, and the pterigopalatine artery was ligated. A filament (nylon monofilament 4/0, Look-sutures; Harvard-Apparatus, Holliston, MA, USA) heat-rounded at the tip was introduced (21 mm) through the external carotid artery to the level where the MCA branches out, and a ligature was placed on the internal carotid artery. Reduction of cerebral blood flow in the MCA territory was confirmed by laser Doppler flowmetry (Table S2). Rats showing a reduction of less than 50% of basal flow were excluded. For reperfusion, the ligature of the internal carotid artery was taken off, and the filament was cautiously removed 45 min after occlusion. Rats were randomized, and researchers were blinded to the treatment after final analysis was completed.

Infarct Size Determination

For infarct size determination, 24 hr after MCAO, magnetic resonance examination was performed using a BIOSPEC BMT 47/40 (Bruker, Ettlingen, Germany; MRI Unit, Instituto Pluridisciplinar, UCM). Infarct volume was calculated using ImageJ 1.41 (NIH, Bethesda, MD, USA) from the T2-weighted images. Additionally, staining of 0.5-mm-thick brain sections with 2,3,5-triphenyltetrazolium chloride (TTC) was used for quantification of brain infarctions on digitalized photographs using ImageJ software.

Long-Term Injury Follow-Up

A subgroup of mice receiving 1 nmol of ApTLR#4FT or ApTLR#4F or vehicle 10 min after pMCAO was used for follow-up of injury progression in the long-term. T2-weighted images were obtained at 24, 48, and 72 hr after MCAO in order to measure sub-acute progression of brain infarction and edema, and mice were terminated at 21 days after MCAO by transcardiac perfusion with 4% paraformaldehyde in 0.1 M phosphate buffer (pH 7.4). Brains were removed and cryoprotected in 0.1 M sucrose in 0.1 M phosphate buffer (pH 7.4). Coronal series were sectioned to a thickness of 30 μm (five sections), each 400 μm and stained with cresyl violet. Injury was expressed as % of reduction of cortical volume by the formula ([vol contralateral cortex − vol remaining ipsilateral cortex]/vol contralateral cortex) × 100.

Long-Term Evaluation of Neurological Function

Footprint patterns were analyzed in mice 21 days after pMCAO using a runway (80 cm long, 10.5 cm wide) with white paper on the bottom. Mouse paws were painted with non-toxic, water-soluble ink of different colors for the hindlimbs and the forelimbs. Stride length, stance length, and sway length (Figure 4E) were measured in five strides per animal.[45,46]

Neurological status in rats was assessed blinded to drug treatment before and at different time points up to 21 days after stroke and by the use of motor and behavioral tests.[47,48]

Fluorescence Microscopy

ApTLR#4FT conjugated with Alexa 488 was injected i.v. in mice 10 min after pMCAO. Unconjugated ApTLR#4FT was used as a negative control. Animals were killed at 24 hr after MCAO by isoflurane overdose followed by transcardiac perfusion through the left ventricle with 0.1 M phosphate buffer as a vascular rinse and by a fixing solution containing 4% p-formaldehyde in 0.1 M phosphate buffer (pH 7.4). Brains were removed, post-fixed overnight, and placed in 30% sucrose for 48 hr. Coronal series were sectioned to a thickness of 30 μm (five sections), each 400 μm. The sections were incubated with an anti-Alexa 488 antibody conjugated to Cy3, and nuclei were counterstained with TO-PRO-3.

In Vivo Neurotoxicity and Measurement of Physiological Parameters

Potential neurotoxicity derived from ApTLR#4FT administration was evaluated by the modified Irwin test, a battery of tests classically used for assessment of the presence of neurotoxic effects derived from drugs. The potential effect of ApTLR4#4FT on general physiological parameters (pH, pCO_2, pO_2, BEEcf [base excess in the extracellular fluid], HCO_3, TCO_2, $sO_2\%$, Na^+, K^+, iCa^{2+}, glucose, hematocrit) was also tested in naive animals (iSTAT SystemBloodAnalyzer, Ven-Bios ES).

Protein Determination by Cytometric Bead Array

Plasma samples obtained 24 hr after pMCAO were used to measure quantitatively the protein levels of IL-6, IL-10, Monocyte Chemoattractant Protein-1 (MCP-1), interferon-γ (IFN-γ), TNF, and IL-12p70 protein levels in a single sample by a BD CBA. This assay allows for the discrimination of different particles based on size and fluorescence. Capture Antibodies (Abs) were covalently coupled to microspheres (beads) according to the manufacturer's instructions (BD Biosciences). Samples in duplicate or standards were added to 75-mm tubes containing 50 μL of mixed capture beads following at 1 hr incubation at room temperature. Then, 50 μL of phycoerythrin (PE) detection reagent (BD Biosciences) was added to each sample or standard tube and left 1 hr at RT. After the incubation, samples and standards were washed with the kit's buffer and centrifuged 5 min at $200 \times g$. Finally, the supernatant was discarded, and another 300 μL of wash buffer were added to each tube. Four-color flow cytometric analysis was performed using a FACSCalibur flow cytometer (BD Biosciences). Data were acquired with the BD CellquestTM PRO and analyzed using the FCAP Array software. FSC versus SSC gating was employed to exclude any sample particles other than the 7.5-μm polystyrene beads. Data were displayed as two-color dot plots (FL-2 versus FL-4) such that the six discrete FL-4 microparticle dye intensities were distributed along the y axis.

Statistics

In all studies, analyses were performed blindly, and randomization was applied. Data are expressed as mean ± SEM for the indicated number of experiments (n is noted in the figure legends). Statistical significance was determined by use of an unpaired Student's t test, of a non-parametric one-way Kruskal-Wallis ANOVA test followed by a Dunn's post hoc test, and of a non-parametric two-way ANOVA followed by Bonferroni post-hoc test as indicated in each figure legend. All statistical analyses were performed with Prism version 5.0 (GraphPad Software, San Diego, CA, USA). $p < 0.05$ was considered statistically significant.

SUPPLEMENTAL INFORMATION

Supplemental Information includes Supplemental Materials and Methods, six figures, and two tables and can be found with this article online at https://doi.org/10.1016/j.ymthe.2018.05.019.

REFERENCES

1. Medzhitov, R. (2001). Toll-like receptors and innate immunity. Nat. Rev. Immunol. *1*, 135–145.

2. Medzhitov, R., Preston-Hurlburt, P., and Janeway, C.A., Jr. (1997). A human homologue of the Drosophila Toll protein signals activation of adaptive immunity. Nature *388*, 394–397.

3. Caso, J.R., Pradillo, J.M., Hurtado, O., Leza, J.C., Moro, M.A., and Lizasoain, I. (2008). Toll-like receptor 4 is involved in subacute stress-induced neuroinflammation and in the worsening of experimental stroke. Stroke *39*, 1314–1320.

4. Caso, J.R., Pradillo, J.M., Hurtado, O., Lorenzo, P., Moro, M.A., and Lizasoain, I. (2007). Toll-like receptor 4 is involved in brain damage and inflammation after experimental stroke. Circulation *115*, 1599–1608.

5. Tang, S.C., Arumugam, T.V., Xu, X., Cheng, A., Mughal, M.R., Jo, D.G., Lathia, J.D., Siler, D.A., Chigurupati, S., Ouyang, X., et al. (2007). Pivotal role for neuronal Toll-like receptors in ischemic brain injury and functional deficits. Proc. Natl. Acad. Sci. USA *104*, 13798–13803.

6. Kanzler, H., Barrat, F.J., Hessel, E.M., and Coffman, R.L. (2007). Therapeutic targeting of innate immunity with Toll-like receptor agonists and antagonists. Nat. Med. *13*, 552–559.

7. Hennessy, E.J., Parker, A.E., and O'Neill, L.A. (2010). Targeting Toll-like receptors: emerging therapeutics? Nat. Rev. Drug Discov. *9*, 293–307.

8. Connolly, D.J., and O'Neill, L.A. (2012). New developments in Toll-like receptor targeted therapeutics. Curr. Opin. Pharmacol. *12*, 510–518.

9. Tuerk, C., and Gold, L. (1990). Systematic evolution of ligands by exponential enrichment: RNA ligands to bacteriophage T4 DNA polymerase. Science *249*, 505–510.

10. Ellington, A.D., and Szostak, J.W. (1992). Selection in vitro of single-stranded DNA molecules that fold into specific ligand-binding structures. Nature *355*, 850–852.

11. Ellington, A.D., and Szostak, J.W. (1990). In vitro selection of RNA molecules that bind specific ligands. Nature *346*, 818–822.

12. White, R.R., Sullenger, B.A., and Rusconi, C.P. (2000). Developing aptamers into therapeutics. J. Clin. Invest. *106*, 929–934.

13. Ramos, E., Piñeiro, D., Soto, M., Abanades, D.R., Martín, M.E., Salinas, M., and González, V.M. (2007). A DNA aptamer population specifically detects Leishmania infantum H2A antigen. Lab. Invest. *87*, 409–416.

14. Bouchard, P.R., Hutabarat, R.M., and Thompson, K.M. (2010). Discovery and development of therapeutic aptamers. Annu. Rev. Pharmacol. Toxicol. *50*, 237–257.

15. Marton, S., Reyes-Darias, J.A., Sánchez-Luque, F.J., Romero-López, C., and Berzal-Herranz, A. (2010). In vitro and ex vivo selection procedures for identifying potentially therapeutic DNA and RNA molecules. Molecules *15*, 4610–4638.

16. Ulrich, H., Trujillo, C.A., Nery, A.A., Alves, J.M., Majumder, P., Resende, R.R., and Martins, A.H. (2006). DNA and RNA aptamers: from tools for basic research towards therapeutic applications. Comb. Chem. High Throughput Screen. *9*, 619–632.

17. Bock, L.C., Griffin, L.C., Latham, J.A., Vermaas, E.H., and Toole, J.J. (1992). Selection of single-stranded DNA molecules that bind and inhibit human thrombin. Nature *355*, 564–566.

18. Rusconi, C.P., Roberts, J.D., Pitoc, G.A., Nimjee, S.M., White, R.R., Quick, G., Jr., Scardino, E., Fay, W.P., and Sullenger, B.A. (2004). Antidote-mediated control of an anticoagulant aptamer in vivo. Nat. Biotechnol. *22*, 1423–1428.

19. Lee, J.H., Canny, M.D., De Erkenez, A., Krilleke, D., Ng, Y.S., Shima, D.T., Pardi, A., and Jucker, F. (2005). A therapeutic aptamer inhibits angiogenesis by specifically targeting the heparin binding domain of VEGF165. Proc. Natl. Acad. Sci. USA *102*, 18902–18907.

20. Martin, J.A., Parekh, P., Kim, Y., Morey, T.E., Sefah, K., Gravenstein, N., Dennis, D.M., and Tan, W. (2013). Selection of an aptamer antidote to the anticoagulant drug bivalirudin. PLoS ONE *8*, e57341.

21. Spiel, A.O., Mayr, F.B., Ladani, N., Wagner, P.G., Schaub, R.G., Gilbert, J.C., and Jilma, B. (2009). The aptamer ARC1779 is a potent and specific inhibitor of von Willebrand Factor mediated ex vivo platelet function in acute myocardial infarction. Platelets *20*, 334–340.

22. Rhodes, A., Deakin, A., Spaull, J., Coomber, B., Aitken, A., Life, P., and Rees, S. (2000). The generation and characterization of antagonist RNA aptamers to human oncostatin M. J. Biol. Chem. *275*, 28555–28561.

23. Du, M., Ulrich, H., Zhao, X., Aronowski, J., and Jayaraman, V. (2007). Water soluble RNA based antagonist of AMPA receptors. Neuropharmacology *53*, 242–251.

24. Pastor, F., Soldevilla, M.M., Villanueva, H., Kolonias, D., Inoges, S., de Cerio, A.L., Kandzia, R., Klimyuk, V., Gleba, Y., Gilboa, E., and Bendandi, M. (2013). CD28 aptamers as powerful immune response modulators. Mol. Ther. Nucleic Acids *2*, e98.

25. Camorani, S., Esposito, C.L., Rienzo, A., Catuogno, S., Iaboni, M., Condorelli, G., de Franiscis, V., and Cerchia, L. (2014). Inhibition of receptor signaling and of glioblastoma-derived tumor growth by a novel PDGFRbeta aptamer. Mol. Ther. *22*, 828–841.

26. Maier, K.E., and Levy, M. (2016). From selection hits to clinical leads: progress in aptamer discovery. Mol. Ther. Methods Clin. Dev. *5*, 16014.

27. Ruckman, J., Green, L.S., Beeson, J., Waugh, S., Gillette, W.L., Henninger, D.D., Claesson-Welsh, L., and Janjić, N. (1998). 2′-Fluoropyrimidine RNA-based aptamers to the 165-amino acid form of vascular endothelial growth factor (VEGF165). Inhibition of receptor binding and VEGF-induced vascular permeability through interactions requiring the exon 7-encoded domain. J. Biol. Chem. *273*, 20556–20567.

28. Wu, C.C., Sabet, M., Hayashi, T., Tawatao, R., Fierer, J., Carson, D.A., Guiney, D.G., and Corr, M. (2008). In vivo efficacy of a phosphodiester TLR-9 aptamer and its beneficial effect in a pulmonary anthrax infection model. Cell. Immunol. *251*, 78–85.

29. Chang, Y.C., Kao, W.C., Wang, W.Y., Wang, W.Y., Yang, R.B., and Peck, K. (2009). Identification and characterization of oligonucleotides that inhibit Toll-like receptor 2-associated immune responses. FASEB J. *23*, 3078–3088.

30. Irwin, S. (1968). Comprehensive observational assessment: Ia. A systematic, quantitative procedure for assessing the behavioral and physiologic state of the mouse. Psychopharmacology (Berl.) *13*, 222–257.

31. Vaure, C., and Liu, Y. (2014). A comparative review of toll-like receptor 4 expression and functionality in different animal species. Front. Immunol. *5*, 316.

32. Hu, J., Wu, J., Li, C., Zhu, L., Zhang, W.Y., Kong, G., Lu, Z., and Yang, C.J. (2011). A G-quadruplex aptamer inhibits the phosphatase activity of oncogenic protein Shp2 in vitro. ChemBioChem *12*, 424–430.

33. Nagatoishi, S., Isono, N., Tsumoto, K., and Sugimoto, N. (2011). Loop residues of thrombin-binding DNA aptamer impact G-quadruplex stability and thrombin binding. Biochimie *93*, 1231–1238.

34. Fujita, H., Imaizumi, Y., Kasahara, Y., Kitadume, S., Ozaki, H., Kuwahara, M., and Sugimoto, N. (2013). Structural and affinity analyses of g-quadruplex DNA aptamers for camptothecin derivatives. Pharmaceuticals (Basel) *6*, 1082–1093.

35. Yamamoto, M., and Takeda, K. (2010). Current views of toll-like receptor signaling pathways. Gastroenterol. Res. Pract. *2010*, 240365.

36. Wang, Y.C., Wang, P.F., Fang, H., Chen, J., Xiong, X.Y., and Yang, Q.W. (2013). Toll-like receptor 4 antagonist attenuates intracerebral hemorrhage-induced brain injury. Stroke *44*, 2545–2552.

37. Hua, F., Tang, H., Wang, J., Prunty, M.C., Hua, X., Sayeed, I., and Stein, D.G. (2015). TAK-242, an antagonist for Toll-like receptor 4, protects against acute cerebral ischemia/reperfusion injury in mice. J. Cereb. Blood Flow Metab. *35*, 536–542.

38. Bustamante, A., Simats, A., Vilar-Bergua, A., García-Berrocoso, T., and Montaner, J. (2016). Blood/brain biomarkers of inflammation after stroke and their association with outcome: from C-reactive protein to damage-associated molecular patterns. Neurotherapeutics *13*, 671–684.

39. Watanabe, T., Ito, K., Matsumoto, M., Seya, T., Nishikawa, S., Hasegawa, T., and Fukuda, K. (2006). Isolation of RNA aptamers against human Toll-like receptor 3 ectodomain. Nucleic Acids Symp. Ser. (Oxf.) *50*, 251–252.

40. Zuker, M. (2003). Mfold web server for nucleic acid folding and hybridization prediction. Nucleic Acids Res. *31*, 3406–3415.

41. Kikin, O., D'Antonio, L., and Bagga, P.S. (2006). QGRS Mapper: a web-based server for predicting G-quadruplexes in nucleotide sequences. Nucleic Acids Res. *34*, W676–W682.

42. Girón, N., Pérez-Sacau, E., López-Fontal, R., Amaro-Luis, J.M., Hortelano, S., Estevez-Braun, A., and de Las Heras, B. (2010). Evaluation of labdane derivatives as potential anti-inflammatory agents. Eur. J. Med. Chem. *45*, 3155–3161.

43. Morancho, A., García-Bonilla, L., Barceló, V., Giralt, D., Campos-Martorell, M., Garcia, S., Montaner, J., and Rosell, A. (2012). A new method for focal transient cerebral ischaemia by distal compression of the middle cerebral artery. Neuropathol. Appl. Neurobiol. *38*, 617–627.

44. Justicia, C., Pérez-Asensio, F.J., Burguete, M.C., Salom, J.B., and Planas, A.M. (2001). Administration of transforming growth factor-alpha reduces infarct volume after transient focal cerebral ischemia in the rat. J. Cereb. Blood Flow Metab. *21*, 1097–1104.

45. Brooks, S.P., and Dunnett, S.B. (2009). Tests to assess motor phenotype in mice: a user's guide. Nat. Rev. Neurosci. *10*, 519–529.

46. Hernández-Jiménez, M., Peña-Martínez, C., Godino, M.D.C., Díaz-Guzmán, J., Moro, M.A., and Lizasoain, I. (2017). Test repositioning for functional assessment of neurological outcome after experimental stroke in mice. PLoS ONE *12*, e0176770.

47. Hunter, A.J., Hatcher, J., Virley, D., Nelson, P., Irving, E., Hadingham, S.J., and Parsons, A.A. (2000). Functional assessments in mice and rats after focal stroke. Neuropharmacology *39*, 806–816.

48. Madrigal, J.L., Caso, J.R., de Cristóbal, J., Cárdenas, A., Leza, J.C., Lizasoain, I., Lorenzo, P., and Moro, M.A. (2003). Effect of subacute and chronic immobilisation stress on the outcome of permanent focal cerebral ischaemia in rats. Brain Res. *979*, 137–145.